CHEMISTRY OF MATERIALS

Article

pubs.acs.org/cm

Synthesis of Zeolites via Interzeolite Transformations without Organic Structure-Directing Agents

Sarika Goel, Stacey I. Zones,*,† and Enrique Iglesia*

Department of Chemical and Biomolecular Engineering, University of California at Berkeley, Berkeley, California 94720, United States

Supporting Information

ABSTRACT: We report synthetic protocols and guiding principles inspired by mechanistic considerations for the synthesis of crystalline microporous solids via interzeolite transformations that avoid direct intervention by organic structure-directing agents. These protocols are specifically implemented to synthesize high-silica MFI (ZSM-5), CHA (chabazite), STF (SSZ-35), and MTW (ZSM-12) zeolites from FAU (faujasite) or BEA (beta) parent materials. These transformations succeed when they lead to daughter structures with higher framework densities, and their nucleation and growth become possible by the presence of seeds or of structural building units common to the parent and target structures, leading, in the latter case, to spontaneous transformations by choosing appropriate synthesis conditions. These protocols allow the synthesis of high-silica frameworks without the use of organic templates otherwise required. The $NaOH/SiO_2$ ratio and Al content in reagents are used to enforce synchronization between the swelling and local restructuring within parent zeolite domains with the spalling of fragments or building units from seeds of the target structure. Seed-mediated interconversions preserve the habit and volume of the parent crystals because of the incipient nucleation of the target structure at the outer regions of the parent domains. The pseudomorphic nature of these transformations requires the concurrent nucleation of mesopores within daughter zeolite crystals because their framework density is larger than that for the parent zeolites. The approach and evidence described shows, for the first time, that a broad range of zeolites rich in silica, and thus more useful as catalysts, can be made without the organic templates originally used to discover them.

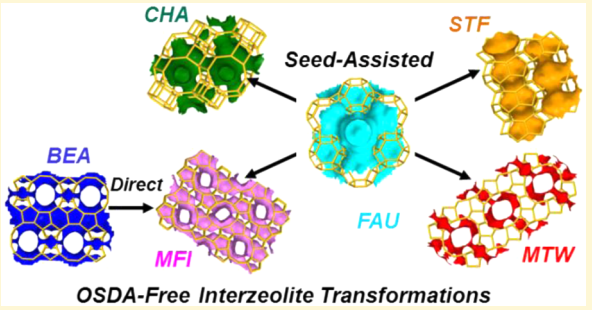

1. INTRODUCTION

Aluminosilicate zeolites are crystalline microporous solids with diverse framework structures and void networks constructed by arrangements of SiO_4^{4-} and AlO_4^{5-} tetrahedral units; these materials are widely used in adsorption, catalysis, and ion-exchange processes.[1−4] Zeolites are typically synthesized by hydrothermal treatment of amorphous aluminosilicate gels in the presence of inorganic (e.g., Na^+, K^+, etc.) and/or organic structure-directing agents (OSDA) in hydroxide or fluoride media.[5−8] OSDA reagents, in particular, increase the cost and the environmental burden of many large-scale zeolite syntheses.

Much effort has been devoted to the development of OSDA-free synthesis protocols to decrease such costs as well the emissions of toxic species in gaseous and water streams generated during the synthesis or subsequent treatments required to decompose organic species contained within zeolite voids. The assembly-disassembly-organization-reassembly (ADOR) mechanism has been developed recently[9,10] as a method of zeolite manipulation without OSDA, in which the selective disassembly of a parent zeolite followed by reassembly can lead to a new topology, but the method is limited in application, as the parent zeolite requires the presence of a hydrolytically sensitive dopant element (e.g., Ge) incorporated within the framework at a specific site, which allows the chemically selective removal of the units containing the dopant. Recently, several groups have reported improved protocols for seed-assisted hydrothermal synthesis of zeolites from amorphous aluminosilicate gels without the use of OSDA species.[11−17] These methods use large concentrations of alkali cations to stabilize the target frameworks and, as a result, have succeeded mostly in the synthesis of Al-rich frameworks (Si/Al < 10). Similar protocols remain unavailable for OSDA-free synthesis of target zeolites (e.g., CHA, STF, MTW, MFI, etc.) with lower Al content, which are often preferred because of their greater structural and acid site stability. In some instances, it has not even been possible to form some target frameworks (e.g., STF, MTW, etc.) with Si/Al ratios below 10.

Zeolites are kinetically (but not thermodynamically) stable toward conversion to denser framework structures (e.g., α-quartz); as a result, their synthesis often involves the formation of structures of intermediate stability in the course of forming the ultimate target structures, which are often rendered stable

Received: December 8, 2014
Revised: February 8, 2015

DOI: 10.1021/cm504510f
Chem. Mater. XXXX, XXX, XXX−XXX

Table 1. Initial Synthesis Molar Compositions, Product Phase, Yield and Final pH of Samples for Synthesis of MFI[a]

sample name	parent zeolite (Si/Al)	$NaOH/SiO_2$[b]	H_2O/SiO_2[b]	time (h)	additional (OSDA/seed)[c]	product phase[d]	product (Si/Al)	final pH	yield[e] (%)
MFI_B-D1	BEA(12.5)	0.35	65	24		Am.			
MFI_B-D2	BEA(37.5)	0.35	65	24		MFI	22	11.8	46
MFI_B-T	BEA(37.5)	0.35	65	24	TPABr (0.05)[f]	MFI	35	12.5	47
MFI_B-S	BEA(37.5)	0.35	65	24	10 wt % MFI seeds	MFI	23	11.8	47
MFI_F-D1	FAU(6)	0.50	95	40		Am.			
MFI_F-D2	FAU(40)	0.50	95	40		Am.			
MFI_F-T	FAU(40)	0.50	95	40	TPABr (0.05)[f]	MFI	33	12.5	58
MFI_F-S1	FAU(40)	0.50	95	40	10 wt % MFI seeds	MFI	22	11.8	47
MFI_F-S2	FAU(40)	0.23	95	40	10 wt % MFI seeds	MFI + Am.	42	11.7	76
MFI_F-S3	FAU(40)	0.85	95	40	10 wt % MFI seeds	MFI	11	12.0	18

[a] T = 423 K for all the syntheses. [b] Reported values excludes the SiO_2 amount present in seed materials. [c] Seed (wt %) = (seed material (g)/parent zeolite (g)) × 100. [d] Am. = amorphous. [e] Yield (%) = [product (g)/(parent zeolite (g) +seed (g))] × 100. [f] Values in parentheses show molar composition of TPABr relative to SiO_2 amount of parent zeolite.

only by the use of specific organic or inorganic cations. Transformations of one zeolite structure into another, interzeolite transformations, have been explored because they can provide a strategy for the selective synthesis of specific structures, often with shorter synthesis times; the mechanistic details of such interzeolite transformations, however, remain unclear,[17−25] and predictions of their success remain largely empirical.

Most reported interconversions use OSDA moieties to induce the nucleation of frameworks that are in fact of lower framework densities and thus less stable than that of the parent zeolite[26,27] or to form structures that would not form at all without the presence of an OSDA.[27,28] Several studies have used seeds to assist the formation of desired structures without the aid of OSDA species,[18,20,22,24,25] and others have induced interzeolite transformations in the presence of both seeds and OSDA.[19,22,28] Successful interzeolite transformations without either seeds or OSDA have been reported only for zeolites with low Si/Al ratios (Si/Al = 4−10);[21−23] to date, target materials with higher Si/Al ratios (Si/Al > 10) do not appear to have been synthesized via interzeolite transformations without the aid of OSDA species.

The present study reports the successful synthesis of high-silica (Si/Al = 11−23) MFI, CHA, STF, and MTW zeolites via OSDA-free interzeolite transformation methods. Parent zeolites BEA (framework density (FD) 15.3; defined as T atom/nm^3, where T stands for Si or Al atoms in the zeolite framework[29]) or FAU (FD 13.3) were transformed into target daughter structures MFI (FD 18.4), CHA (FD 15.1), STF (FD 16.9), or MTW (FD 18.2) via recrystallization in aqueous NaOH under hydrothermal conditions. Structures with lower framework densities were successfully transformed into more stable structures with higher framework densities. Concomitant kinetic hurdles required the presence of a common composite building unit (CBU) between parent and target structures or, in their absence, the addition of either seeds or OSDA moieties for successful transformations.

We propose a plausible synthesis mechanism, pseudomorphic in nature, for seed-assisted transformations that is consistent with the observed effects of the parent Si/Al ratio, the $NaOH/SiO_2$ ratio, and the required synthesis temperature and time, as well as with the crystal habit and intracrystal mesoporous voids in the daughter structures. The resulting concepts and strategies provide predictive guidance for synthesizing a broad range of zeolite frameworks in the direction dictated by thermodynamics and with kinetics mediated by either common structural units along the reaction coordinate or by seeds of the target product.

2. EXPERIMENTAL SECTION

2.1. Reagents and Materials. Fumed SiO_2 (Cab-O-Sil, HS-5, 310 m^2 g^{-1}), NaOH (99.995%, Sigma-Aldrich), FAU (CBV780, Zeolyst, Si/Al = 40, H-FAU), FAU (CBV712, Zeolyst, Si/Al = 6, NH_4^+-FAU), BEA (CP811E-75, Zeolyst, Si/Al = 37.5, H-BEA), BEA (CP814E, Zeolyst, Si/Al = 12.5, NH_4^+-BEA), and tetrapropylammonium bromide (TPABr, 98%, Sigma-Aldrich) were used as received.

2.2. Synthesis Procedures. *2.2.1. MFI, CHA, STF, and MTW Seeds.* The materials used as seeds were prepared using previously described synthesis procedures for MFI (S_1),[30] CHA,[31] STF,[32] and MTW[33] zeolites. MFI (S_2) was synthesized by dissolving $Al(OH)_3$ (53% Al_2O_3, Reheis F-2000 dried gel, 0.44 g) in a solution containing deionized H_2O (38 g), tetrapropylammonium hydroxide (TPAOH, 40 wt %, Aldrich, 7.5 g), and KOH (1 M solution in deionized H_2O, Fisher, 15 g). Ludox AS-30 colloidal silica (18 g) was added to the solution, and the mixture was then transferred into a Teflon-lined stainless steel autoclave (Parr, 125 cm^3) and held at 423 K for 3 days under static conditions. The resulting solids were collected by filtration through a fritted disc Buchner filter funnel (Chemglass, 150 mL, F) and washed with deionized water (17.9 MΩ·cm resistivity) until the rinse liquids reached a pH of 8−9, and the sample was heated in a forced convection oven at 373 K overnight.

2.2.2. Synthesis of MFI via Transformations of BEA or FAU Zeolites. In a typical synthesis, zeolite BEA or FAU was added (0.5−1.0 g) to an aqueous NaOH solution, into which the MFI seed crystals or organic structure-directing agents (TPABr) were added to prepare final mixtures with molar compositions listed in Table 1. These mixtures were placed within sealed polypropylene containers (Nalgene, 125 cm^3) and homogenized by vigorous magnetic stirring (400 rpm; IKA RCT Basic) for 1 h at ambient temperature. The mixture was then transferred into a Teflon-lined stainless steel autoclave and held at 423 K for 24−40 h under static conditions. The resulting solids were collected by filtration through a fritted disc Buchner filter funnel (Chemglass, 150 mL, F) and washed with deionized water (17.9 MΩ·cm resistivity) until the rinse liquids reached a pH of 8−9. The sample was heated in a forced convection oven at 373 K overnight. The solid yields of the resulting products were defined as

$$\text{yield (\%)} = \frac{\text{product (g)}}{\text{parent zeolite (g)} + \text{seeds (g)}} \times 100 \quad (1)$$

The samples were then treated in a tube furnace in flowing dry air (1.67 cm^3 g^{-1} s^{-1}) to 773 K at 0.03 K s^{-1} and held at this temperature for 3 h. The samples, after treatment, were denoted MFI_B-D, MFI_B-T, and MFI_B-S when synthesized from BEA and MFI_F-D, MFI_F-T, and

DOI: 10.1021/cm504510f
Chem. Mater. XXXX, XXX, XXX−XXX

Table 2. Initial Synthesis Molar Compositions, Product Phase, Yield, and Final pH of Samples for Transformations of FAU Using CHA, STF, and MTW Seeds[a]

sample name	parent (Si/Al)	$NaOH/SiO_2$[b]	seeds[c] (10 wt %)	temp (K)	product phase[d]	product (Si/Al)	final pH	yield[e] (%)	crystallinity (%)
CHA_F-S1	FAU(40)	0.50	CHA	423	CHA + Am.	19	11.8	46	50
CHA_F-S2	FAU(40)	0.68	CHA	423	CHA + Am.	11	11.7	25	66
CHA_F-S3	FAU(40)	0.85	CHA	423	CHA + MOR		12.2	22	
CHA_F-S4	FAU(40)	0.50	CHA	428	CHA + Am.		11.9	49	
STF_F-S1	FAU(40)	0.50	STF	423	STF + Am.		11.8	47	
STF_F-S2	FAU(40)	0.50	STF	428	STF + Am.		11.8	48	
STF_F-S3	FAU(40)	0.50	STF	433	STF + MFI		12.0	52	
STF_F-S4	FAU(40)	0.68	STF	423	STF + Am.	11	11.7	26	78
STF_F-S5	FAU(40)	0.85	STF	423	STF + MOR		12.0	33	
MTW_F-S1	FAU(40)	0.50	MTW	423	MTW + Am.		11.9	44	
MTW_F-S2	FAU(40)	0.50	MTW	428	MTW + Am.		11.8	48	
MTW_F-S3	FAU(40)	0.68	MTW	423	MTW + Am.	12	12.0	29	60

[a] H_2O/SiO_2 = 95, and synthesis time = 40 h for all syntheses. [b] Reported values exclude the SiO_2 amount present in seed materials. [c] Seed (wt %) = (seed material (g)/parent zeolite (g)) × 100. [d] Am. = amorphous. [e] Yield (%) = (product (g)/(parent zeolite (g) + seed (g))) × 100.

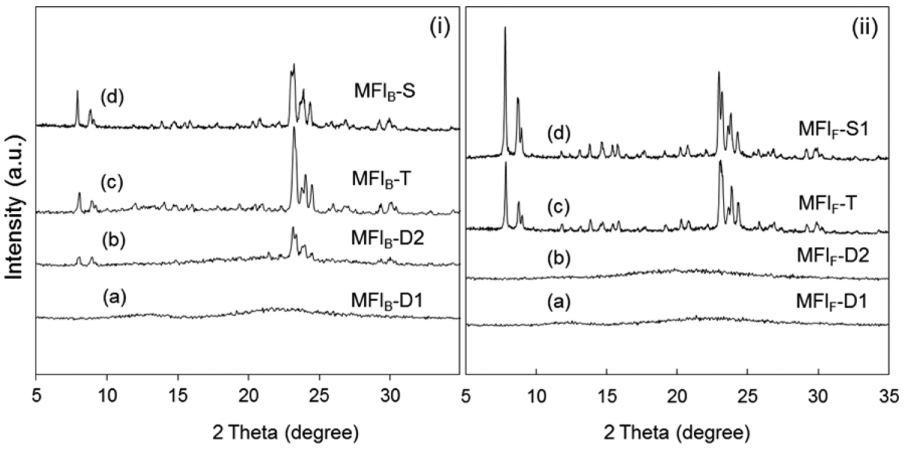

Figure 1. X-ray diffractograms of the products synthesized from parent (i) BEA and (ii) FAU via (a, b) direct, (c) template-assisted, and (d) seed-assisted (using MFI seeds (S_1)) transformations. Syntheses were carried out at 423 K, $NaOH/SiO_2$ = 0.35 (from BEA) and 0.50 (from FAU), and H_2O/SiO_2 = 65 (from BEA) and 95 (from FAU) (Table 1).

MFI_F-S when synthesized from FAU in the direct (-D), template-assisted (-T), and seed-assisted (-S) transformations, respectively.

2.2.3. Synthesis of CHA, STF, and MTW via Transformations of FAU. The synthesis of CHA, STF, and MTW zeolites was achieved by transformations of FAU as parent material. FAU (0.5−1.0 g) was added to an aqueous NaOH solution to achieve molar compositions of xNaOH: 1.0 SiO_2: 0.0125 Al_2O_3: 95 H_2O (x = 0.50, 0.68, 0.85), into which 10 wt % (weight percent based on parent FAU) seed crystals (CHA, STF, or MTW) were added to prepare final mixtures with molar compositions listed in Table 2. These mixtures were placed within sealed polypropylene containers (Nalgene, 125 cm^3) and homogenized by vigorous magnetic stirring (400 rpm; IKA RCT Basic) for 1 h at ambient temperature. These mixtures were then transferred into a Teflon-lined stainless steel autoclave and held at the desired crystallization temperature (423, 428, or 433 K) for 40 h under static conditions. The resulting solids were collected by filtration through a fritted disc Buchner filter funnel (Chemglass, 150 mL, F) and washed with deionized water (17.9 MΩ·cm resistivity) until the rinse liquids reached a pH of 8−9. The samples were heated in a forced convection oven at 373 K overnight. The samples were then treated in tube furnace in flowing dry air (1.67 $cm^3\ g^{-1}\ s^{-1}$) to 873 K at 0.03 K s^{-1} and held at this temperature for 10 h. The resulting samples after treatment were denoted CHA_F-S, STF_F-S, and MTW_F-S, synthesized via transformations of FAU using seeds of CHA, STF, and MTW, respectively.

For the synthesis of the H-form of these zeolites, the treated Na-zeolite samples were added to an aqueous NH_4NO_3 solution (>98%, Sigma-Aldrich, 1 g zeolite per 100 cm^3 of 0.1 M solution) while stirring at 353 K for 4 h. The solids were recovered by filtration, and this process was repeated two more times to yield NH_4-zeolite. The resulting samples were then treated in tube furnace in flowing dry air (1.67 $cm^3\ g^{-1}\ s^{-1}$) to 873 K at 0.03 K s^{-1} and held at this temperature for 3 h to form H-zeolite.

2.3. Characterization of Framework Structures and Crystallinity. The identity and phase purity of the product zeolites were demonstrated by powder X-ray diffraction (XRD) measurements (Cu Kα radiation λ = 0.15418 nm, 40 kV, 40 mA, Bruker D8 Advance). Diffractograms were collected for 2θ values of 5−35° at 0.02° intervals with a 2 s scan time. The crystallinity was calculated using MgO as an internal standard in powder XRD. The ratio of the sum of areas of three major peaks in the target material to that of their corresponding seed material (100% crystalline) was defined as the percentage crystallinity of each sample. Si, Al, and Na contents of the samples were measured by inductively coupled plasma atomic emission spectroscopy (ICP-AES) (IRIS Intrepid spectrometer; Galbraith Laboratories). Transmission electron microscope (TEM) images were taken on Philips/FEI Tecnai 12 microscope operated at 120 kV. Before TEM analysis, the samples were suspended in ethanol and dispersed onto ultrathin carbon/holey carbon films supported on 400 mesh Cu grids (Ted Pella Inc.). Nitrogen and argon adsorption−desorption measurements of zeolite products were performed on ASAP 2020 (Micromeritics) at 77 and 87 K, respectively. Prior to the measurements, all samples were degassed at 623 K for 4 h under vacuum. The final pH values were measured at ambient temperature

DOI: 10.1021/cm504510f
Chem. Mater. XXXX, XXX, XXX−XXX

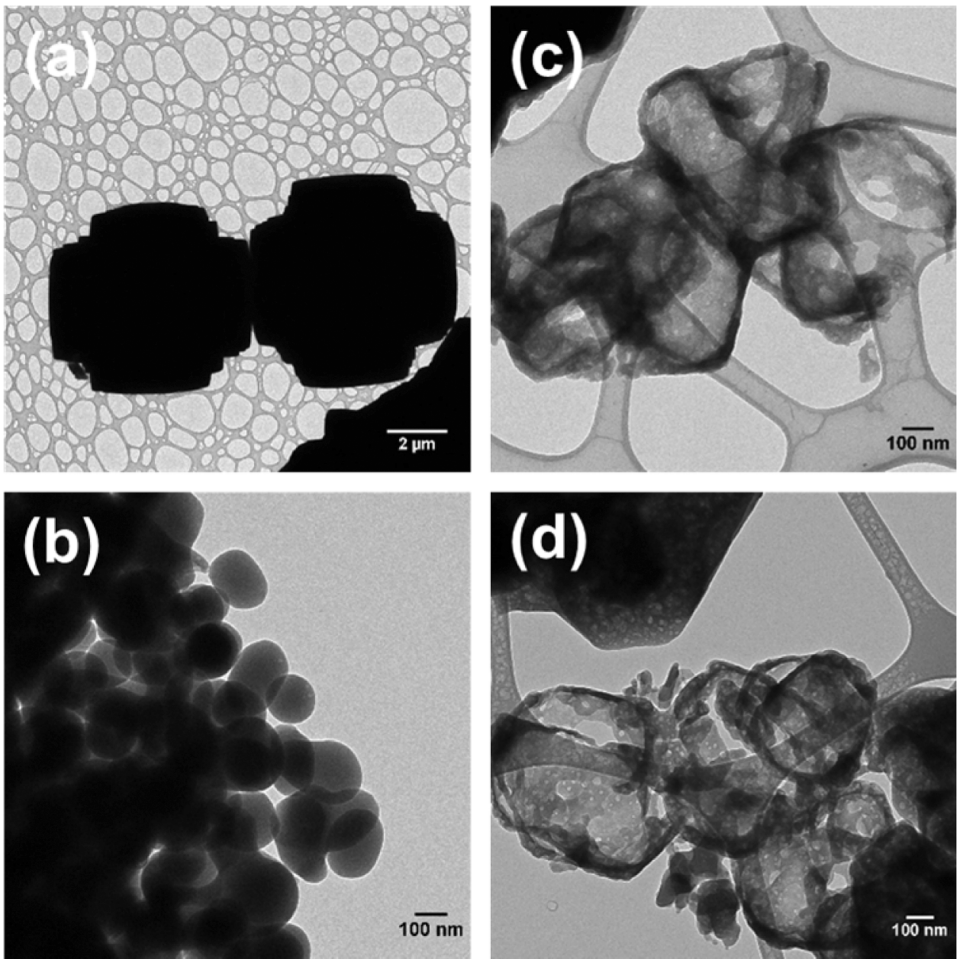

Figure 2. TEM images of MFI seeds (a) S_1 (~6 μm) and (b) S_2 (~0.2 μm) and products synthesized via transformations of parent FAU (Si/Al = 40) using (c) S_1 and (d) S_2 MFI seeds. The syntheses were carried out at 423 K, $NaOH/SiO_2$ = 0.5, H_2O/SiO_2 = 95 for 40 h with 10 wt % MFI seeds.

using an Orion Ross combination electrode (Orion 8103BNUMP) with an Orion Star A215 meter (calibrated using buffer solutions of pH 7.00, 10.01, and 12.00).

3. RESULTS AND DISCUSSION

3.1. Synthesis of MFI via Transformations of Parent BEA. Parent BEA zeolites with low Si content (Si/Al = 12.5) formed only amorphous solids in aqueous NaOH ($NaOH/SiO_2$ = 0.35, H_2O/SiO_2 = 65; Table 1) at 423 K under hydrothermal conditions (X-ray diffractogram; Figure 1(i)a); MFI frameworks preferentially form in gels with high Si/Al contents because abundant five-membered rings in MFI are disfavored at high Al contents.[34]

MFI crystals readily formed, however, from parent BEA zeolites with lower Al contents (Si/Al = 37.5; X-ray diffractogram; Figure 1(i)b, 46% yield (eq 1); Table 1) in aqueous NaOH solution ($NaOH/SiO_2$ = 0.35, H_2O/SiO_2 = 65; Table 1) under autogenous pressures at 423 K. Interestingly, this transformation occurred spontaneously, without requiring the presence of either seeds or OSDA. The Si/Al ratio in the MFI product (Si/Al = 22; Table 1) was lower than in the parent BEA (Si/Al = 37.5), and the solids yield was 46% (Table 1), suggesting that nearly all of the Al in the parent BEA was incorporated into the product MFI, whereas some SiO_2 remained dissolved in solution at the high final pH (11.8, Table 1). Crystalline MFI was obtained also from template-assisted (with TPABr) and seed-assisted (with 10 wt % MFI seeds (S_1)) transformations of parent BEA (Si/Al = 37.5) (X-ray diffractograms; Figure 1(i)c, 1(i)d, 47% yield (eq 1) for both; Table 1). Thus, we conclude that parent BEA zeolites with high Si content (Si/Al = 37.5) successfully transformed to MFI spontaneously and in the presence of either MFI seeds or OSDA (TPABr) at Si/Al ratios in the parent BEA that favor MFI frameworks.

We note that the framework structures and CBU of the parent BEA and product MFI include a common *mor* structural motif.[29] It seems plausible, therefore, that a CBU, present in BEA and required to form MFI, remains essentially intact within BEA-derived intermediates during the conversion of BEA to MFI; this CBU may assist the local nucleation of MFI and, in doing so, minimize inherent kinetic hurdles and allow BEA to MFI transformations to occur without seeds or OSDA. This common CBU may serve as a kinetic mediator[12,30] for nucleating the daughter structure, suggesting that zeolites containing common CBU may be able to overcome kinetic barriers that impede their interconversions in the direction dictated by the thermodynamic tendency of zeolites to form structures with greater framework densities. MFI zeolites were obtained after 24 h from parent BEA zeolites (Figure 1(i)), whereas hydrothermal MFI syntheses from amorphous aluminosilicate gels, with or without OSDA, typically require 2−15 days.[35] Thus, the presence of the BEA structure, plausibly

DOI: 10.1021/cm504510f
Chem. Mater. XXXX, XXX, XXX−XXX

because of its common CBU with MFI, shortens synthesis times because of rapid nucleation.

Next, we explore the implications of this common CBU hypothesis for assisting nucleation of target frameworks, first by attempting the synthesis of MFI from FAU, within which a common CBU is absent, under similar conditions that led to the spontaneous transformation of BEA into MFI. From these resulting observations, we propose a set of requirements for successful zeolite interconversions and the validation of these guidelines by the synthesis of CHA, STF, and MTW zeolites from parent FAU zeolite.

3.2. Synthesis of MFI via Transformations of Parent FAU. Parent FAU zeolites with Si/Al ratios of 6 and 40 gave only amorphous solids in hydrothermal aqueous NaOH environments ($NaOH/SiO_2$ = 0.5, H_2O/SiO_2 = 95; Table 1) at 423 K (X-ray diffractograms; Figure 1(ii)a,(ii)b), consistent with kinetic hurdles that cannot be overcome despite favorable thermodynamics (FAU, FD 13.3; MFI, FD 18.4), possibly because of the lack of a common CBU. MFI formed, however, when FAU (Si/Al = 40) was treated in similar hydrothermal environments but with TPABr (OSDA) or MFI seeds in the synthesis mixture (X-ray diffractograms; Figure 1(ii)c,(ii)d, 58 and 47% yield (eq 1), respectively; Table 1). These findings contrast the ability of BEA precursors to form MFI even in the absence of such kinetic mediation as OSDA or seeds, which are required in the case of parent FAU zeolites, to assist the nucleation of the favored MFI structures. These data, taken together, provide compelling but circumstantial evidence for the role of common CBU motifs in assisting nucleation in lieu of the more frequent strategies that use OSDA or seeds as the nucleation sites or centers.

Figure 2 shows TEM images of two MFI seed materials of different crystal size (~6 μm, seed S_1; Figure 2a and ~0.2 μm, seed S_2; Figure 2b) and of the MFI products formed from FAU parent zeolites using each of these seeds (Figure 2c,d, respectively). The crystal habit and size of the MFI products using S_1 (TEM, Figure 2c) and S_2 (TEM, Figure 2d) seeds are similar (~0.7 μm diameter) and differ markedly from those of the MFI seeds used (TEM, Figure 2a,b), which do not remain intact as they mediate MFI nucleation from parent FAU crystals. These seeds do not serve as intact nucleation sites but instead provide CBU species or shed small fragments, as in the case of homogeneous nucleation and growth during seed-assisted hydrothermal synthesis from amorphous aluminosilicate gels.[6,28] The products crystals are in fact smaller (~0.7 μm crystals, Figure 2c) than the S_1 seed crystals (~6 μm crystals, Figure 2a), making epitaxial growth[6,28] of MFI crystals onto seeds implausible.

FAU diffraction lines disappeared after synthesis times of 4 h, whereas MFI lines were detectable at all times (4–40 h; Figure 3a–f) in transformations of FAU using MFI seeds (S_1). The amorphous background in the diffractograms (Figure 3; 2θ = 20–30°) disappeared and the MFI diffraction lines became the only discernible features after 24 h. These data indicate that FAU crystals lose their long-range order in NaOH media within a time scale that still preserves the identity of MFI seeds, which provide essential components for the ultimate recrystallization of FAU parent structures into MFI.

The size and shape of MFI crystals formed from seed-assisted FAU conversion to MFI did not change significantly during synthesis (4–40 h; TEM; Figure 4b–f) and resemble those of the parent FAU zeolite (TEM; Figure 4a). MFI mean crystal sizes are only slightly larger than those in the FAU parent

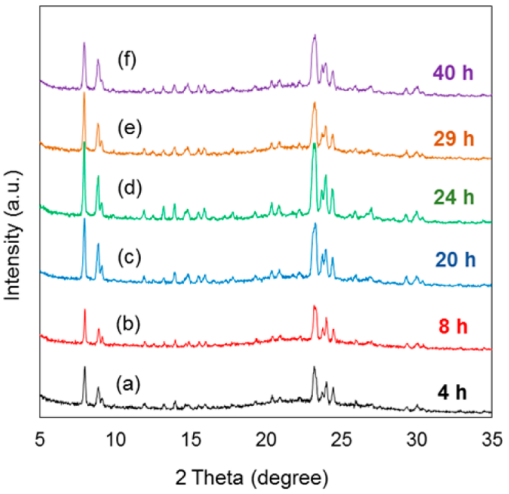

Figure 3. X-ray diffractograms of the products synthesized via seed-assisted transformations of parent FAU (Si/Al = 40) at synthesis times of (a) 4, (b) 8, (c) 20, (d) 24, (e) 29, and (f) 40 h. Syntheses were carried out at 423 K, $NaOH/SiO_2$ = 0.5, H_2O/SiO_2 = 95 with 10 wt % MFI seeds (S_1).

zeolites (crystal size histograms; Figure 5). These findings would be consistent with a seed-assisted growth mechanism in which FAU structures loosen to form structures without local order and spalled MFI fragments from MFI seeds induce the nucleation of MFI frameworks at their outer surfaces, thus fixing an outer crust that allow it to preserve the habit and size of the parent crystals (Scheme 1). Such volume-conserving (pseudomorphic) transformations reflect the exclusive contact of seed fragments with the outer surface of locally disrupted, but otherwise intact, FAU domains, which nucleate MFI from the outer to the inner regions of these FAU domains.

The pseudomorphic nature of these processes requires the nucleation of voids in order to account for higher framework density of MFI relative to FAU. Such voids are evident in the TEM images of the product crystals (Figure 4b–f). The mechanistic hypothesis depicted in Scheme 1 would suggest that successful transformations require the synchronization of the local disruption of the FAU structure and the shedding of nucleating fragments from the MFI seeds. The requirement for high-silica FAU parent zeolites to form high-silica MFI products further implicates such synchronization because the lower solubility of higher Al-content FAU structures may preclude local disruptions before the complete dissolution and loss of the local structures and CBU moieties of the MFI seeds (Si/Al ~ 300). The full dissolution of either FAU or MFI before interactions between seed fragments and locally disrupted FAU domains would prevent these seed-assisted pseudomorphic transformations.

The crystallinity of the MFI products calculated from the resulting diffractograms (with MgO as an internal standard) was 98%. The micropore volume from nitrogen adsorption data was 0.116 cm^3/g for MFI products (from MFI seeds (S_2)), similar to the pore volume of MFI seeds S_2 (0.12 cm^3/g) measured by the same method. Ar adsorption–desorption measurements on MFI crystals from seed-assisted transformations of FAU (using MFI seeds (S_1)) show hysteresis behavior at P/P_o (P_o is the saturation pressure at 87 K) values of ~0.4 (Figure 6), indicative of capillary condensation within mesopores;[37,38] such behavior is not observed for MFI seed materials prepared by hydrothermal synthesis using structure-

DOI: 10.1021/cm504510f
Chem. Mater. XXXX, XXX, XXX–XXX

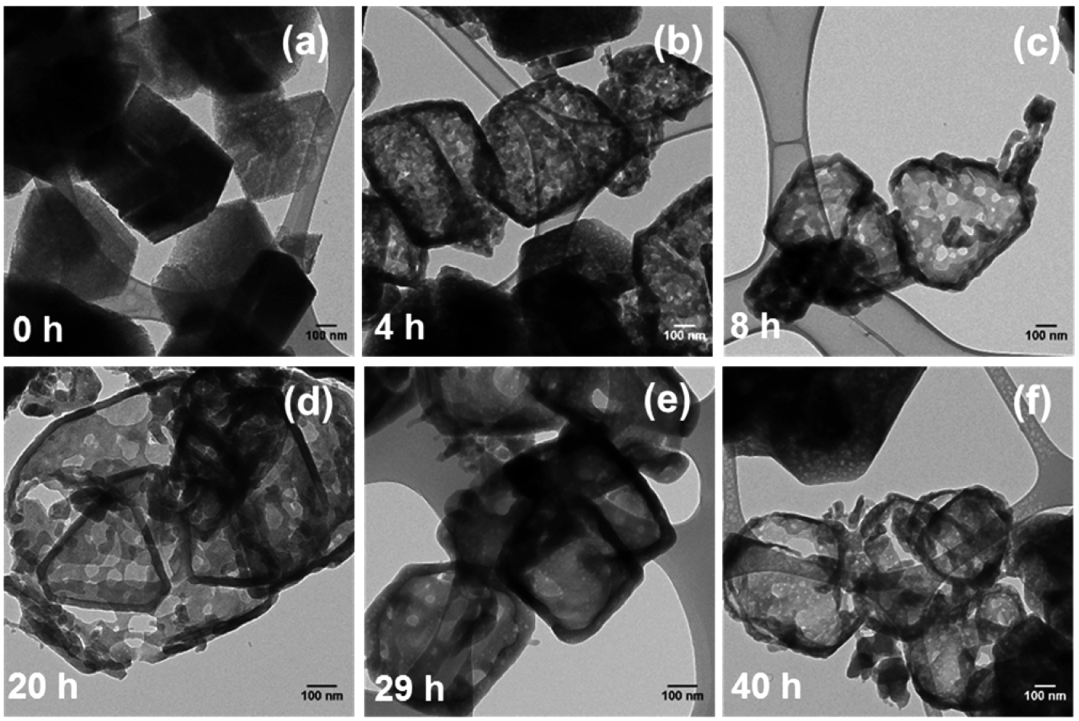

Figure 4. TEM images of the products synthesized via seed-assisted transformations of parent FAU (Si/Al = 40) at synthesis times of (a) 0 (parent FAU), (b) 4, (c) 8, (d) 20, (e) 29, and (f) 40 h. Syntheses were carried out at 423 K, $NaOH/SiO_2$ = 0.5, H_2O/SiO_2 = 95 with 10 wt % MFI seeds (S_1).

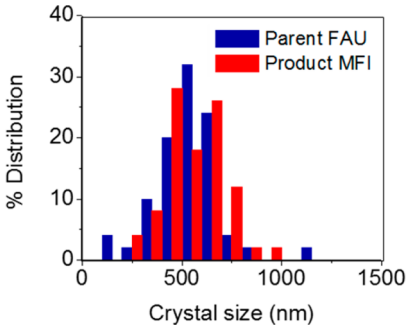

Figure 5. Crystal size distributions of parent FAU and product MFI zeolites (MFI_F-S1) synthesized via seed-assisted transformations of FAU (Si/Al = 40). The synthesis was carried out at 423 K, $NaOH/SiO_2$ = 0.5, H_2O/SiO_2 = 95 for 40 h with 10 wt % MFI seeds (S_1).

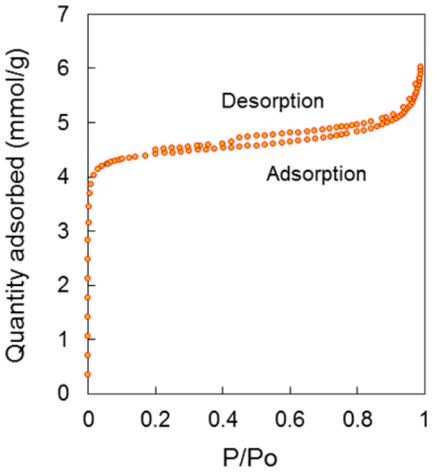

Figure 6. Ar adsorption and desorption isotherms for the product MFI zeolite (MFI_F-S1) synthesized via seed-assisted transformations of FAU (Si/Al = 40). The synthesis was carried out at 423 K, $NaOH/SiO_2$ = 0.5, H_2O/SiO_2 = 95 for 40 h with 10 wt % MFI seeds (S_1).

Scheme 1. Schematic Representation of the Proposed Mechanism for Seed-Assisted Transformations of Parent FAU to Daughter MFI zeolites

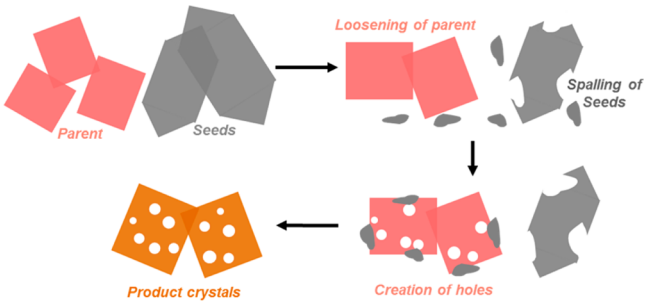

directing agents (TPABr; Section 2.2.1). Thus, we conclude that seed-assisted FAU to MFI transformations lead to the formation of mesopores directly during MFI crystallization, without requiring post-synthesis desilication.[37] Such mesopores are useful in practice because they decrease the diffusion distances prevalent for intact crystals; they also provide compelling evidence for the pseudomorphic (space-conserving) nature of seed-assisted interzeolite transformations.

We conclude that FAU-derived species retain their physical integrity, but as quasi-amorphous domains, and that incipient nucleation occurs at the outer regions of such domains by spalled subunits or CBU species derived from MFI seeds, which retain the local MFI structure required to assist the transformation of FAU-derived domains into MFI crystals. The space-conserving nature of the transformation requires, in turn,

DOI: 10.1021/cm504510f
Chem. Mater. XXXX, XXX, XXX−XXX

the nucleation of mesoscopic voids within the formed MFI crystals because their framework density is higher than that of the parent FAU. Any premature full dissolution of either seeds or parent zeolite into amorphous silica−alumina gels would prevent such seed-assisted interzeolite transformations, as we show in the next section, in which we propose a set of specific guidelines for successful transformations based on these mechanistic insights and on the observed spontaneous BEA conversion into MFI. Then, we assess the validity and usefulness of these guidelines by carrying out the synthesis of high-silica CHA, STF, and MTW zeolites via transformations of FAU and by varying the relevant synthesis conditions so as to achieve the intended transformations.

3.3. Requirements for Successful Zeolite Interconversions. The findings and mechanistic inferences described thus far have suggested that successful interzeolite transformations require (i) favorable thermodynamics—a parent zeolite of lower framework density than the target structure; (ii) a kinetic route to the target structure—nucleation assisted by either a common CBU between parent and target zeolites or seeds of the target zeolite; (iii) synthesis conditions that favor the target structure, instead of alternate structures, when common CBU are used to assist the transformation; (iv) high Si/Al parent zeolites when high-silica target structures are sought to allow complete conversion of locally amorphous parent domains; (v) synchronization of the spalling of the fragments or CBU moieties from seeds and the swelling and local restructuring of parent zeolite domains; (vi) $NaOH/SiO_2$ and Si/Al ratios that balance solubilization of seeds and parent zeolites so as to enforce synchronization in (v); and (vii) chemical composition of the gel and synthesis conditions conducive to the formation of only the desired target structure in highly crystalline form.

FAU to MFI transformations were attempted for a range of $NaOH/SiO_2$ ratios (0.23 and 0.85 compared to 0.50 in Section 3.2) to probe the effects of synchronization or lack thereof between the local restructurings of the parent and seed zeolites. Diffractograms showed that $NaOH/SiO_2$ ratios of 0.23 led to essentially amorphous solids with only trace amounts of MFI crystals. In contrast, $NaOH/SiO_2$ ratios of 0.50 (Section 3.2) and 0.85 gave highly crystalline solids (98 and 100%, respectively). The lower solid yields achieved at higher $NaOH/SiO_2$ ratios (from 47 to 18% for $NaOH/SiO_2$ ratios of 0.50 and 0.85, respectively; Table 1), and the concomitant lower Si/Al ratios in MFI products (from 22 to 11; Table 1) indicate that a substantial fraction of SiO_2 in the parent FAU and the MFI seeds dissolved at the high final pH (12.0, Table 1) prevalent in synthesis protocols at the highest $NaOH/SiO_2$ ratio (0.85; Table 1). Such findings are consistent with the premature dissolution of one or both precursors before seed-derived MFI fragments contact locally disrupted FAU structures in the parent zeolite crystals.

Next, we explore the extension of these mechanism-based guidelines to the synthesis of high-silica CHA (FD 15.1), STF (FD 16.9), and MTW (FD 18.2) zeolites via interzeolite transformations of FAU (FD 13.3) and the synthesis conditions required for the effective synchronization required for successful transformations.

3.3.1. Synthesis of CHA via Transformations of FAU. CHA (FD 15.1) has a denser framework structure than FAU (FD 13.3) and contains a common *d6r* CBU; thus, we surmise that their interconversion can proceed without the assistance of seeds. As a result, we have attempted to form high-silica crystalline CHA from transformations of FAU under the same synthesis conditions as those used in transformations of FAU to MFI.

FAU (Si/Al = 40) formed only amorphous solids in the absence of seeds (0.5 NaOH: 1.0 SiO_2: 0.0125 Al_2O_3: 95 H_2O; Table 1), as shown in Figure 1, indicating that these synthesis conditions are not conducive to CHA formation. Thus, the synthesis condition was changed to that used previously[17] for synthesis of CHA from amorphous aluminosilicate gel, although without the use of an organic structure-directing agent. Crystalline CHA products with high Al content (Si/Al ∼ 2.5) were obtained (X-ray diffraction patterns; Figure S1) by transformations of high Al FAU (Si/Al = 2.5) in aqueous KOH under these conditions (KOH/SiO_2 = 0.54, H_2O/SiO_2 = 20, 403 K). The use of NaOH or of high-silica FAU, however, did not lead to the spontaneous formation of CHA (X-ray diffraction patterns; Figure S1), suggesting that both K^+ and high Al FAU are required for spontaneous transformations of FAU into CHA and that there are significant kinetic barriers that prevent the formation of Na-CHA or high-silica CHA in the absence of seeds or OSDA species.

The use of CHA seeds with FAU parent zeolites with low Al contents may, however, circumvent the difficult nucleation suggested by the formation of amorphous structures in the presence of only common CBU species. Challenges may persist, though, as seed-assisted strategies require synchronization between the spalling of small structures or CBU species from CHA seeds and the local disruption of the FAU parent crystals. The addition of 10 wt % CHA seeds (0.5 NaOH: 1.0 SiO_2: 0.0125 Al_2O_3: 95 H_2O; Table 2) to FAU (Si/Al = 40) led to the formation of crystalline CHA zeolite (Si/Al = 19) after 40 h at 423 K (Figure 7) under conditions similar to those used for seed-assisted synthesis of MFI from FAU. The yield of solids (46%; Table 2) was similar to that measured for direct BEA to MFI conversion or seed-assisted FAU to MFI conversion (46−47%; Table 1). These similar yields reflect the solution equilibrium[39] under the synthesis conditions, which dissolves excess Si species, and result in similar yields (∼47%) in all cases. The solids formed contain some amorphous materials, as shown by the broad background in their diffractograms (2θ = 20−30°; Figure 7), in contrast with the absence of substantial amorphous solids in the MFI products formed from BEA or FAU parent zeolites.

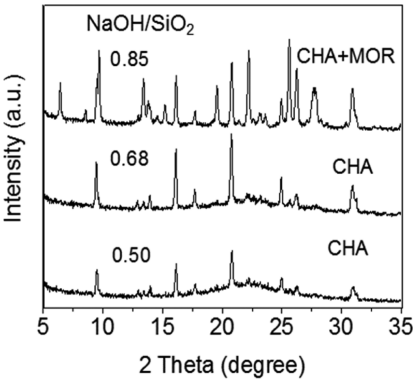

Figure 7. X-ray diffractograms of the products synthesized via transformations of FAU (Si/Al = 40) at $NaOH/SiO_2$ ratios of (a) 0.50, (b) 0.68, and (c) 0.85 using 10 wt % CHA seeds. Syntheses were carried out at 423 K, H_2O/SiO_2 = 95 for 40 h (Table 2).

DOI: 10.1021/cm504510f
Chem. Mater. XXXX, XXX, XXX−XXX

Higher $NaOH/SiO_2$ ratios (0.68 vs 0.50; Figure 7) led to CHA products with higher crystallinity (66 vs 50%; Table 2), possibly because the concomitantly higher pH favors faster disruptions of both CHA seeds and FAU parent crystals (without resulting in a full dissolution of FAU or of CHA seeds), leading to more effective synchronization. The solids yield and Si/Al ratio of the products formed (Table 2), in turn, decreased from 46 to 25% and 19 to 11, respectively, when $NaOH/SiO_2$ ratios increased from 0.50 to 0.68 because of the higher amounts of SiO_2 species dissolved in the liquid phase at the higher pH in the silica-rich synthesis gel. In contrast, amorphous aluminosilicate gels under similar synthesis conditions (0.68 NaOH: 1.0 SiO_2: 0.0125 Al_2O_3: 95 H_2O) with 10 wt % CHA seeds led to a mixture of CHA and MOR zeolites as products with only 6% yield (Figure S2), confirming that the parent FAU zeolites in these interzeolite transformations do not dissolve completely and form amorphous aluminosilicate species.

CHA products were 66% crystalline, measured by powder XRD using MgO as an internal standard (Table 2); yet, the micropore volume, obtained from N_2 adsorption measurements, of these CHA products was 0.094 cm^3/g (per g of total solids), which is smaller than the theoretical void space of CHA (0.242 cm^3/g, ref 36), consistent with the presence of some amorphous solids in the final material but inconsistent with the crystallinity measurements from XRD. The H-CHA sample, synthesized by ammonium ion exchange of Na-CHA sample followed by thermal treatment in air to remove NH_3 (Section 2.2.3), showed no significant differences in the amount of nitrogen adsorbed (micropore volume 0.095 cm^3/g, Table S1) compared to that of Na-CHA, suggesting that the pore blocking is not caused by localization of alkali cations at the pore entrances but perhaps by the presence of amorphous solids that can lead to a narrowing of pore openings or extra framework debris that can cause pore filling.

Formation of amorphous solids may reflect the imperfect synchronization of the local disruption of the FAU crystals and the disintegration of CHA seeds into nucleating moieties, a likely consequence of the higher Al content (and lower solubility) of CHA seeds (Si/Al = 15) compared with those in the FAU parent zeolite (Si/Al = 40) and the seeds used in MFI synthesis (Si/Al ~ 300) from FAU; the higher Al content in CHA seeds could delay the spalling of nucleation centers to a point after the parent FAU crystals lose their structural integrity. Thus, higher $NaOH/SiO_2$ ratios, which increase the solubility of CHA seeds without dissolving the parent FAU completely, may achieve more effective synchronization. A further increase in $NaOH/SiO_2$ ratio (to 0.85) leads to the formation of mixtures of CHA and MOR phases (Figure 7), indicating that high synthesis pH values lead to faster incipient nucleation of several frameworks as a result of the premature dissolution of parent or seed materials and rapid growth, thus making such high pH conditions inappropriate for the selective synthesis of a single zeolite framework. Thus, the synthesis of high-silica CHA (Si/Al = 11) was achieved from transformations of FAU with CHA seeds using the developed synthesis guidelines; further investigations are needed, however, to understand the low micropore volume from nitrogen adsorption measurements in the final CHA products leading to the blocking of some pores. Next, we discuss the synthesis of high-silica STF and MTW zeolites via transformations of FAU based on the proposed synthesis guidelines for the success of these transformations.

3.3.2. Synthesis of STF via Transformations of FAU. STF structures are denser than FAU and thus thermodynamically favored, but these two frameworks do not share a common CBU, suggesting that FAU transformations into STF would require the assistance of STF seeds.

FAU (Si/Al = 40) formed only amorphous solids in the absence of any seeds under the synthesis conditions used (0.5 NaOH: 1.0 SiO_2: 0.0125 Al_2O_3: 95 H_2O; Table 1), as shown in Figure 1. STF zeolites, however, formed in synthesis mixtures containing parent FAU zeolite (Si/Al = 40) and 10 wt % STF seeds (Si/Al = 20) after 40 h at 423 K, conditions similar to those used for FAU to MFI transformations (0.5 NaOH: 1.0 SiO_2: 0.0125 Al_2O_3:95 H_2O; Table 2), but the solids formed were of lower crystallinity than in the case of MFI (Figure 8 and Table 2). Higher $NaOH/SiO_2$ ratios (0.68 and 0.85 vs 0.50) led to more crystalline STF solids, similar to the pH effects observed in seed-assisted CHA synthesis from FAU (Figure 7). At the 0.68 $NaOH/SiO_2$ ratio, high-silica STF (Si/Al = 11) formed (Figure 9a) with solid yields of 26% (Table 2), similar to those measured in seed-assisted FAU conversion to CHA (Si/Al = 11, 25% yield, Table 2). The STF product was 78% crystalline, measured by powder XRD using MgO as an internal standard (Table 2); yet, its micropore volume (from N_2 adsorption) was 0.027 cm^3/g (Table S1), a value much smaller than the theoretical value for STF structure (0.20 cm^3/g, ref 36). Possible reasons for the low micropore volumes and

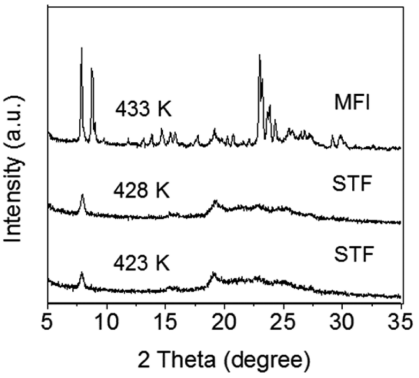

Figure 8. X-ray diffractograms of the products synthesized via transformations of parent FAU (Si/Al = 40) at various temperatures in the presence of 10 wt % STF seeds. Syntheses were carried out for 40 h at $NaOH/SiO_2$ = 0.5, H_2O/SiO_2 = 95 (Table 2).

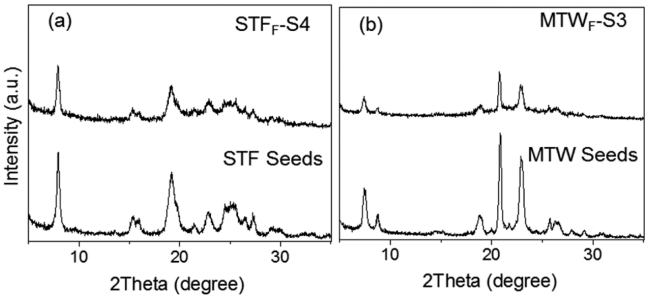

Figure 9. X-ray diffractograms of the products synthesized via transformations of parent FAU (Si/Al =40) with 10 wt % seeds of (a) STF and (b) MTW and their corresponding seeds used. Syntheses were carried out at 423 K, $NaOH/SiO_2$ = 0.68, H_2O/SiO_2 = 95 for 40 h (Table 2).

DOI: 10.1021/cm504510f
Chem. Mater. XXXX, XXX, XXX−XXX

efforts to increase the pore volume of the STF sample are discussed in the next section.

Higher temperatures (428 K) in seed-assisted FAU conversions to STF did not cause detectable changes in the intensity of STF diffraction lines (Figure 8) or in the product yield or Si/Al ratio (Table 2). Further increase in the temperature (433 K) led to the formation of the denser MFI structures instead of STF (Figure 8), suggesting that STF crystals derived from FAU with the assistance of seeds are metastable and form MFI by overcoming kinetic hurdles to form denser structures at higher temperatures. STF and MFI zeolites share the *cas* structural motif, suggesting that *cas* moieties in STF seeds or in STF crystals formed from FAU can also assist MFI nucleation from parent FAU crystals at these higher temperatures.

The synthesis of high-silica STF (Si/Al = 11) was achieved from transformations of FAU using STF seeds; the STF products showed micropore volume lower than that expected from the STF crystal structure and the XRD crystallinity data; we explore plausible causes and potential solutions for this low micropore volume accessibility in STF products in the next section. First, we discuss the synthesis of high-silica MTW zeolites via transformations of FAU.

3.3.3. Synthesis of MTW via Transformations of FAU. MTW structures are also denser than FAU and thus thermodynamically favored, but they do not share a common CBU with FAU; thus, we expect that FAU conversion to MTW will require the presence of MTW seeds in the synthesis mixture. Indeed, FAU (Si/Al = 40) formed only amorphous solids in the absence of any seeds under the synthesis conditions used (0.5 NaOH: 1.0 SiO_2: 0.0125 Al_2O_3: 95 H_{2O}; Table 1), as shown previously in Figure 1. MTW zeolites formed in synthesis mixtures containing parent FAU zeolites (Si/Al = 40) and 10 wt % MTW (Si/Al = 30) seeds after 40 h at 423 K under conditions similar to those used for FAU to MFI, CHA, and STF transformations (0.5 NaOH: 1.0 SiO_2: 0.0125 Al_2O_3: 95 H_2O; Table 2), but the solids formed had significant amorphous phase present, similar to that for STF and CHA syntheses. High-silica MTW (Si/Al = 12) formed, from transformation of FAU using MTW seeds, with solid yield of 29% (Table 2) at a $NaOH/SiO_2$ ratio of 0.68 (Figure 9), similar to those measured for seed-assisted FAU conversion to CHA (Si/Al = 11, 25% yield, Table 2) and STF (Si/Al = 11, 26% yield, Table 2). This MTW product was 60% crystalline (Table 2), measured by powder XRD using MgO as an internal standard, but the micropore volume (from N_2 adsorption) was 0.006 cm^3/g (Table S1), much smaller than the theoretical value for MTW structure (0.11 cm^3/g, ref 36) and inconsistent with the relatively higher crystallinity value obtained from XRD measurements.

The small values of accessible micropore volumes (Table S1) in the STF and MTW zeolites formed via seed-assisted synthesis from FAU are not consistent with their crystalline nature and may reflect ubiquitous channel blockages that have been reported for one-dimensional zeolites, such as STF and MTW. Previous studies on MOR zeolites[40,41] have concluded that such blockages account for the inability of MOR structures (with 0.65 × 0.70 nm channels along the [001] direction and 0.57 × 0.26 nm along the [011] direction) to adsorb molecules with kinetic diameters larger than ~0.4 nm;[40] such blockages have been attributed to intrachannel amorphous debris and to cations or defects along the main channels in MOR. These factors may also account for the low accessible micropore volumes reported here for STF and MTW zeolites.

H-STF and H-MTW samples, prepared by exchanging the seed-assisted Na-STF and Na-MTW samples with NH_4^+ cations and treatment in air at 873 K (Section 2.2.3), did not lead to higher N_2 uptake than that of the Na-containing samples (micropore volumes; Table S1). We conclude that any channel blockages are not caused by Na cations but may reflect instead the presence of amorphous intrachannel debris or structural defects that may form within the one-dimensional channels during crystal growth. The extensive twinning and faulting in MTW frameworks, caused by the incoherent stacking of polymorphs, have been reported in MTW prepared via OSDA-assisted[42] and OSDA-free[15] protocols from amorphous aluminosilicate gels. Stacking faults may also form during synthesis without OSDA, but such effects cannot be detected via powder XRD due to their local nature and their small number. Further studies are currently underway using magic angle spinning (MAS) NMR and high-resolution electron microscopy (HREM) to better understand the reduced micropore volume behavior of these materials.

The metastable nature of seed-mediated synthesis products (toward conversion to denser structures) was confirmed by examining the evolution of various crystalline structures with increasing synthesis time. Products from transformations of FAU using MFI, CHA, STF, or MTW seeds converted to denser structures as time proceeded and led to mixtures of dense zeolite phases after 10 days of synthesis (X-ray diffraction patterns; Figure S3).

Next, we test one of the proposed guidelines for the kinetic route to the target zeolite: nucleation assisted by either a common CBU between parent and product zeolites or seeds of the desired zeolite help to overcome the kinetic barriers during transformations by probing the conversion of FAU and BEA zeolite mixture into the product MFI, where BEA can either generate the *mor* CBU common with MFI or directly transform to MFI seeds (as described in Section 3.1), which can promote the transformation of FAU.

3.3.4. Synthesis of MFI via Transformations of FAU and BEA Zeolite Mixtures. BEA converts to MFI in the absence of MFI seeds or OSDA, but either seeds or OSDA are required to successfully form MFI from FAU, apparently because of their lack of a common CBU. The presence of small amounts of BEA in a mixture with the parent FAU zeolite may allow the in situ formation of either MFI seed crystals or *mor* structural units (from BEA).

Indeed, MFI formed from FAU−BEA mixtures (50−50 wt %) regardless of whether MFI seeds were present (10 wt %; Figure 10a) or not (Figure 10b) ($NaOH/SiO_2$ = 0.45, H_2O/SiO_2 = 80). MFI structures formed even for 5 or 10 wt % BEA in such mixtures (Figure 10c,d). MFI product yields (46−48%) were similar to those observed in spontaneous BEA to MFI transformation and seed-assisted FAU to MFI interconversions (46−47%, Table 1). These data show that BEA assists the nucleation of MFI structures from FAU, through its ability to lower kinetic barriers in FAU to MFI transformations by providing either *mor* structural units (common to MFI) or MFI seed crystals. In this manner, the on-purpose synthesis and addition of seeds of the target structure (or OSDA requirements) are avoided, in general, by exploiting a spontaneous transformation of a minority component of a zeolite with a common CBU with the target zeolite to effect the conversion of a parent zeolite that lacks a common CBU with the target

DOI: 10.1021/cm504510f
Chem. Mater. XXXX, XXX, XXX−XXX

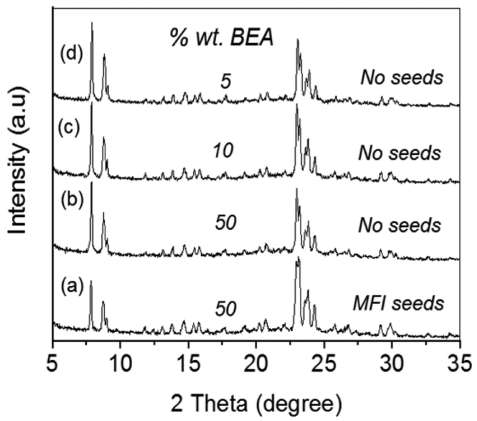

Figure 10. X-ray diffractograms of the products synthesized via transformations of FAU and BEA in (a) a mixture with 50% BEA and assisted by MFI seeds and seed-free mixtures with (b) 50%, (c) 10%, and (d) 5% BEA. Syntheses were carried out at 423 K, $NaOH/SiO_2$ = 0.45, H_2O/SiO_2 = 80 and 40 h with/without 10 wt % MFI seeds (S_1).

framework structure. This general strategy is consistent with the guidelines developed in the previous sections and shows that target seeds and/or common CBU can be formed in situ, thus avoiding the specific addition of target seeds to parent zeolites that require kinetic assistance because of the lack of a common CBU with target structures.

These data, together with the effect of synthesis temperature, confirm that products of the interzeolite transformations are metastable structures for a certain set of synthesis conditions; these structures, with time or temperature, will convert to thermodynamically more stable structures (dense phases). These transformations, taken together, provide evidence for the key role of the Si/Al ratio of the parent zeolite in determining their ability to restructure and form high-silica zeolites, of NaOH to SiO_2 ratios of the synthesis gel to ensure the synchronized decomposition of the parent and the seed structures, and of temperature and time to form metastable desired structures. The successful synthesis of high-silica CHA, STF, and MTW zeolites supports the validity of the synthesis guidelines; further investigations for pore unblocking are, however, required to form accessible highly crystalline products. We expect that the interzeolite transformation protocols developed here for the synthesis of high-silica zeolites can be extended further to zeolites of different frameworks, void environments, and framework compositions, based on their framework density and CBU components. These methods not only synthesize zeolites without OSDA but also form mesoporous crystals, which are known to improve the accessibility of reactant molecules to the zeolite micropores[41] in chemical reactions catalyzed within such micropores and thus have the potential to enhance the turnover rates and tune the selectivity to desired products.

4. CONCLUSIONS

We have demonstrated a general strategy and a set of guiding rules for the synthesis of microporous solids without the use of organic structure-directing agents (OSDA) via interzeolite transformation protocols. Parent structures with lower framework densities (FAU or BEA) were successfully transformed into thermodynamically favored more stable structures with higher framework densities (MFI, CHA, STF, and MTW) via recrystallization in aqueous NaOH under hydrothermal conditions. Successful transformations required that we overcome kinetic hurdles while exploiting the thermodynamic tendency of microporous solids to increase their framework density. Transformation of BEA to MFI occurred spontaneously without any significant kinetic and thermodynamic hurdles, whereas the conversion of FAU to MFI, CHA, STF, and MTW required the product seeds, suggesting the absence of sufficient kinetic driving forces in these cases. A plausible synthesis mechanism, pseudomorphic in nature (transformations that conserve the volume occupied by the parent crystals, leading to similar size and crystal shape in products), for seed-assisted transformations is consistent with the observed effects of the parent Si/Al ratio, the $NaOH/SiO_2$ ratio, and the required synthesis temperature and time, as well as with the crystal habit and intracrystal mesoporous voids in the product crystals. Such phenomena reflect incipient nucleation of new structures occurring at the outer regions of the parent crystals and leading to the formation of mesoporosity during such transformations as a natural consequence of the space-conserving nature of the structural changes and of the higher density of the daughter frameworks. Specific guidelines for successful transformations are inferred from the mechanistic insights of seed-assisted FAU to MFI transformation and from the spontaneous BEA conversion into MFI. The findings and mechanistic inferences suggest that successful interzeolite transformations require (i) favorable thermodynamics—a parent zeolite of lower framework density than the target structure; (ii) a kinetic route to the target structure—nucleation assisted by either a common CBU between parent and target zeolites or seeds of the target zeolite; and (iii) chemical composition of gel and synthesis conditions conducive to the formation of only the desired target structure, instead of alternate structures, in highly crystalline form. The synthesis mechanism and the guidelines developed here enable us to design the synthesis conditions required for desired zeolites, which previously required OSDA for the synthesis, and will expand the diversity of framework types of zeolites that can be synthesized via these methods.

■ ASSOCIATED CONTENT

Ⓢ Supporting Information

X-ray diffraction patterns and micropore volumes of samples synthesized via interzeolite transformations of FAU using MFI, CHA, STF, and MTW seeds at various synthesis conditions. This material is available free of charge via the Internet at http://pubs.acs.org.

■ AUTHOR INFORMATION

Corresponding Authors

*(S.I.Z.) E-mail: sizo@chevron.com.
*(E.I.) E-mail: iglesia@berkeley.edu. Fax: (510) 642−4778.

Present Address

†(S.I.Z.) Chevron Energy Technology Company, Richmond, California 94801, United States.

Notes

The authors declare the following competing financial interest(s): (1) The funding for the research came from Chevron Energy and Technology Co. and (2) Stacey I. Zones is an employee of this company and, more generally, is also a stockholder in Chevron Corp.

DOI: 10.1021/cm504510f
Chem. Mater. XXXX, XXX, XXX−XXX

■ ACKNOWLEDGMENTS

We thank Reena Zalpuri (Electron Microscope Lab) for help with the TEM instrument, Dr. Prashant Deshlahra, Stanley Herrmann, Edwin Yik, and Dr. Xueyi Zhang for the careful review of this manuscript, and Chevron Energy Technology Company for the financial support for this research.

■ REFERENCES

(1) Davis, M. E. *Chem. Mater.* **2014**, *26*, 239−245.
(2) Weisz, P. B.; Frilette, V. J.; Maatman, R. W.; Mower, E. B. *J. Catal.* **1962**, *1*, 307−312.
(3) Csicsery, S. M. *Zeolites* **1984**, *4*, 202−213.
(4) Barrer, R. M. In *Zeolite Synthesis*; Occelli, M. L., Robson, H. E., Eds.; American Chemical Society: Washington, DC, 1989; Vol. *398*, pp 11−27.
(5) Corma, A.; Davis, M. E. *ChemPhysChem* **2004**, *5*, 304.
(6) Cundy, C. S.; Cox, P. A. *Microporous Mesoporous Mater.* **2005**, *82*, 1−78.
(7) Moliner, M.; Martínez, C.; Corma, A. *Chem. Mater.* **2014**, *26*, 246−258.
(8) Meng, X.; Xiao, F.-S. *Chem, Rev.* **2014**, *114*, 1521−1543.
(9) Roth, W. J.; Nachtigall, P.; Morris, R. E.; Wheatley, P. S.; Seymour, V. R.; Ashbrook, S. E.; Chlubná, P.; Grajciar, L.; Položij, M.; Zukal, A.; Shvets, O.; Čejka, J. *Nat. Chem.* **2013**, *5*, 628.
(10) Wheatley, P. S.; Chlubná-Eliášová, P.; Greer, H.; Zhou, W.; Seymour, V. R.; Dawson, D. M.; Ashbrook, S. E.; Pinar, A. B.; McCusker, L. B.; Opanasenko, M.; Čejka, J.; Morris, R. E. *Angew. Chem., Int. Ed.* **2014**, *53*, 13210.
(11) Xie, B.; Zhang, H.; Yang, C.; Liu, S.; Ren, L.; Zhang, L.; Meng, X.; Yilmaz, B.; Müller, U.; Xiao, F.-S. *Chem. Commun.* **2011**, *47*, 3945−3947.
(12) Itabashi, K.; Kamimura, Y.; Iyoki, K.; Shimojima, A.; Okubo, T. A. *J. Am. Chem. Soc.* **2012**, *134*, 11542−11549.
(13) Iyoki, K.; Itabashi, K.; Okubo, T. *Microporous Mesoporous Mater.* **2014**, *189*, 22.
(14) Iyoki, K.; Itabashi, K.; Chaikittisilp, W.; Elangovan, S. P.; Wakihara, T.; Kohara, S.; Okubo, T. *Chem. Mater.* **2014**, *26*, 1957.
(15) Kamimura, Y.; Iyoki, K.; Elangovan, S. P.; Itabashi, K.; Shimojima, A.; Okubo, T. *Microporous Mesoporous Mater.* **2012**, *163*, 282.
(16) Kamimura, Y.; Itabashi, K.; Okubo, T. *Microporous Mesoporous Mater.* **2012**, *147*, 149.
(17) Moden, B.; Cooper, D.; Li, H. X.; Cormier, W. E. U.S. Patent 0269719A1, 2012.
(18) Zones, S. I. *J. Chem. Soc., Faraday Trans.* **1991**, *87*, 3709−3716.
(19) Itakura, M.; Goto, I.; Takahashi, A.; Fujitani, T.; Ide, Y.; Sadakane, M.; Sano, T. *Microporous Mesoporous Mater.* **2011**, *144*, 91−96.
(20) Honda, K.; Itakura, M.; Matsuura, Y.; Onda, A.; Ide, Y.; Sadakane, M.; Sano, T. *J. Nanosci. Nanotechnol.* **2013**, *13*, 3020−3026.
(21) Nedyalkova, R.; Montreuil, C.; Lambert, C.; Olsson, L. *Top. Catal.* **2013**, *56*, 550−557.
(22) Sano, T.; Itakura, M.; Sadakane, M. *J. Jpn Pet. Inst.* **2013**, *56*, 183−197.
(23) Tendeloo, L. V.; Gobechiya, E.; Breynaert, E.; Martens, J. A.; Kirschhock, C. E. A. *Chem. Commun.* **2013**, *49*, 11737−11739.
(24) Jon, H.; Ikawa, N.; Oumi, Y.; Sano, T. *Chem. Mater.* **2008**, *20*, 4135−4141.
(25) Honda, K.; Yashiki, A.; Sadakane, M.; Sano, T. *Microporous Mesoporous Mater.* **2014**, *196*, 254.
(26) Dhainaut, J.; Daou, T. J.; Bidal, Y.; Bats, N.; Harbuzaru, B.; Lapisardi, G.; Chaumeil, H.; Defoin, A.; Rouleau, L.; Patarin. *CrystEngComm* **2013**, *15*, 3009−3015.
(27) Maldonado, M.; Oleksiak, M. D.; Chinta, S.; Rimer, J. D. *J. Am. Chem. Soc.* **2013**, *135*, 2641.
(28) Oleksiak, M. D.; Rimer, J. D. *Rev. Chem. Eng.* **2013**, *30*, 1.
(29) Baerlocher, C.; McCusker, L. B. Database of zeolite structures; http://www.iza-structure.org/databases/.
(30) Goel, S.; Zones, S.; Iglesia, E. *J. Am. Chem. Soc.* **2014**, *136*, 15280.
(31) Zones, S. I. Patent US8007763B2, August 30, 2011.
(32) Musilová-Pavlačková, Z.; Zones, S. I.; Čejka, J. *Top. Catal.* **2010**, *53*, 273.
(33) Jones, A. J.; Zones, S. I.; Iglesia, E. *J. Phys. Chem. C* **2014**, *118*, 17787.
(34) Martens, J. A.; Jacobs, P. A. *Synthesis of High-Silica Aluminosilicate Zeolites*; Elsevier: New York, 1987.
(35) Auerbach, S. M.; Carrado, K. A.; Dutta, P. K. *Handbook of Zeolite Science and Technology*; M. Dekker: New York, 2003.
(36) Calero Diaz, S. In *Zeolites and Catalysis*; Čejka, J., Corma, A., Zones, S., Eds.; Wiley-VCH: Weinheim, Germany, 2010; pp 335−360.
(37) Lee, P.-S.; Zhang, X.; Stoeger, J. A.; Malek, A.; Fan, W.; Kumar, S.; Yoo, W. C.; Al Hashimi, S.; Penn, R. L.; Stein, A.; Tsapatsis, M. *J. Am. Chem. Soc.* **2011**, *133*, 493.
(38) Sing, K. S. W.; Everett, D. H.; Haul, R. a. W.; Moscou, L.; Pierotti, R. A.; Rouquerol, J.; Siemieniewska, T. In *Handbook of Heterogeneous Catalysis*; Ertl, G., Ed.; Wiley-VCH: Weinheim, Germany, 2008.
(39) Iler, R. K. *The Chemistry of Silica: Solubility, Polymerization, Colloid and Surface Properties and Biochemistry of Silica*; Wiley: New York, 1979.
(40) Raatz, F.; Marcilly, C.; Freund, E. *Zeolites* **1985**, *5*, 329.
(41) Möller, K.; Bein, T. *Chem. Soc. Rev.* **2013**, *42*, 3689.
(42) Ritsch, S.; Ohnishi, N.; Ohsuna, T.; Hiraga, K.; Terasaki, O.; Kubota, Y.; Sugi, Y. *Chem. Mater.* **1998**, *10*, 3958.

DOI: 10.1021/cm504510f
Chem. Mater. XXXX, XXX, XXX−XXX